Using Dimensional Analysis to Assess Scalability and Accuracy in Molecular Communication

Adam Noel*†, Karen C. Cheung*, and Robert Schober*†
*Department of Electrical and Computer Engineering
University of British Columbia, Email: {adamn, kcheung, rschober}@ece.ubc.ca
†Institute for Digital Communications
University of Erlangen-Nürnberg, Email: {noel, schober}@LNT.de

***Abstract*—In this paper, we apply dimensional analysis to study a diffusive molecular communication system that uses diffusing enzymes in the propagation environment to mitigate intersymbol interference. The enzymes bind to information molecules and then degrade them so that they cannot interfere with the detection of future transmissions at the receiver. We determine when it is accurate to assume that the concentration of information molecules throughout the receiver is constant and equal to that expected at the center of the receiver. We show that a lower bound on the expected number of molecules observed at the receiver can be arbitrarily scaled over the environmental parameters, and generalize how the accuracy of the lower bound is qualitatively impacted by those parameters.**

I. Introduction

Molecular communication, where a transmitter sends information by emitting molecules into its surrounding environment to be carried to a receiver, is a popular candidate for implementation in networks where communicating devices have functional components that are on the order of nanometers in size, i.e., nanonetworks. Such networks can take advantage of the inherent biocompatibility of using molecules as information carriers, since living organisms already do so; see [1, Ch. 16]. Advancements in nanotechnology will enable a wide range of applications using bio-hybrid components that communicate using molecules, as described in detail in [2], [3].

Free diffusion is a simple propagation method for molecules since no external energy is required and no new infrastructure is needed between communicating devices. However, the data transmission rate decreases as the receiver is placed further away from the transmitter. In addition, communication capacity is limited by the proximity of molecules over time as they randomly diffuse. A receiver may be unable to differentiate between the arrival of the same type of molecule emitted at different times, i.e., it can observe intersymbol interference (ISI). Despite these drawbacks, many researchers have adopted free diffusion for the design of molecular communication networks, cf. e.g. [4]–[8].

Since ISI is a major bottleneck to the performance of diffusive molecular communication, actively reducing the lingering presence of information molecules can significantly improve capacity. For example, information molecules can be transformed as they diffuse so that they are no longer recognized by the receiver. Specifically, enzymes diffusing in the propagation environment can be used to repeatedly transform information molecules because of their selectivity and because the enzymes are not consumed by the reaction mechanism.

In [9], we introduced a model for analyzing diffusive molecular communication systems that have enzymes present throughout the entire propagation environment. By reacting with the information molecules, the enzymes improve performance; they reduce the "tail" effect created by diffusing molecules that linger near the receiver. In [9], we presented a lower bound expression for the expected number of information molecules observed at a receiver placed some distance from a transmitter that emits impulses of molecules.

In this paper, we provide a dimensionless model for analyzing diffusive molecular communication systems that have diffusing enzymes. Dimensional analysis facilitates comparison between different dimensional parameter sets with the use of reference parameters and the creation of dimensionless constants (please refer to [10] for more on dimensional analysis). Using a dimensionless model generalizes the model's scalability. Specifically, we can verify the accuracy of our lower bound expression by simulating small environments to save computational resources and then arbitrarily extrapolate the results to larger environments.

Furthermore, the dimensionless model facilitates an exact study of the applicability of the uniform concentration assumption, where the concentration of information molecules throughout the receiver is assumed to be constant and equal to that expected at the center of the receiver. This assumption simplifies analysis and is often made explicitly (as in [5], [9]) or implicitly (by assuming a point receiver, as in [6]–[8]). However, analysis of the accuracy of this assumption has not yet been performed in the molecular communications literature. Assessing the assumption's validity will instill confidence in its continued use.

Dimensional analysis was applied in this paper to make the following contributions:

1) For the case of diffusion only (no active enzymes present), we derive the expected dimensionless number of information molecules observed at the receiver from emission by a point source but without the assumption of uniform concentration of those molecules within the receiver volume. We consider cubic and spherical volumes and use numerical results to gain insight into

when the uniform concentration assumption is accurate.
2) We show that the lower bound on the expected number of observed information molecules at the receiver when enzymes are present can be arbitrarily scaled over parameters that include the size and placement of the receiver, the chemical reactivity of the molecular species, and the number of molecules.
3) We generalize the accuracy of the lower bound expression on the expected number of information molecules at the receiver when enzymes are present. The qualitative impact of the environmental parameters on the accuracy is considered.

The rest of this paper is organized as follows. In Section II, we describe the dimensionless model for transmission between a single transmitter and receiver. The exact expected number of information molecules for the case of diffusion only, where we do not apply the uniform concentration assumption, is derived in Section III. In Section IV, we show the scalability and accuracy of the lower bound expression on the number of molecules at the receiver when enzymes are present. Numerical and simulation results are presented in Section V. We make our conclusions in Section VI.

II. Physical Model

In this section, we briefly describe our physical model as we introduced in [9] before we define reference parameters to translate the model into dimensionless form.

A. Dimensional Form

The transmitter is fixed at the origin of an unbounded 3-dimensional aqueous environment. The receiver is an observer with a fixed volume of size V_{obs}, centered at location $\{x_0, y_0, z_0\}$ where $\vec{r}_0$ is the vector from the origin to $\{x_0, y_0, z_0\}$, and of arbitrary shape.

We are interested in three mobile species: A molecules, E molecules, and EA molecules. A molecules are the information molecules that are released by the transmitter. These molecules have a negligible natural degradation rate but they are able to act as substrates with enzyme E molecules. We apply the Michaelis-Menten reaction mechanism (a common mechanism for enzymes; see [11]) to the A and E molecules:

$$E + A \xrightarrow{k_1} EA, \tag{1}$$

$$EA \xrightarrow{k_{-1}} E + A, \tag{2}$$

$$EA \xrightarrow{k_2} E + A_P, \tag{3}$$

where EA is the intermediate formed by the binding of an A molecule to an enzyme molecule, A_P is the degraded A molecule that is not recognized by the receiver (so we can ignore them once created), and k_1, k_{-1}, and k_2 are the reaction rates for the reactions as shown with units molecule^{-1}m^3 s^{-1}, s^{-1}, and s^{-1}, respectively. Reaction (3) degrades A molecules irreversibly while the enzymes are released intact, enabling the latter to participate in future reactions.

The number of molecules of species S is given by N_S, and its concentration at the point defined by vector $\vec{r}$ and at time t in molecule $\cdot$ m^{-3} is $C_S(\vec{r}, t)$. For compactness, we will sometimes write $C_S(\vec{r}, t) = C_S$. We assume that every molecule of each species S diffuses independently of all other molecules with diffusion constant D_S defined as [12, Eq. 4.16]

$$D_S = \frac{k_B T}{6\pi\eta R_S}, \tag{4}$$

where k_B is the Boltzmann constant ($k_B = 1.38 \times 10^{-23}$ J/K), T is the temperature in kelvin, η is the viscosity of the medium in which the particle is diffusing ($\eta \approx 10^{-3}$ kg $\cdot$ m^{-1}s^{-1} for water at 25 °C), and R_S is the molecule radius. Thus, the units for D_S are m^2/s.

The transmitter communicates by emitting impulses of A molecules, where the number of molecules emitted is N_A (not to be confused with Avogadro's Number). The receiver counts the number of unbound A molecules that are within the receiver volume but has no influence on any of the reaction or diffusion processes. Using a passive receiver without specifying a detection mechanism enables us to focus on the propagation behaviour. N_E E molecules are initially randomly (uniformly) distributed throughout a finite cubic volume V_{enz} that includes both the transmitter and receiver with the transmitter at the center. V_{enz} is impermeable to E molecules (so that we can simulate using a finite number of E molecules) but not A molecules (EA molecules decompose to their constituents if they hit the boundary). Thus, the *total* concentration of the free and bound enzyme in V_{enz}, $C_{E_{Tot}}$, is constant and equal to N_E/V_{enz}. V_{enz} is sufficiently large to assume in analysis that it is infinite in size.

B. Dimensionless Form

For dimensional analysis we define reference variables; please refer to [10] for more on dimensional analysis. We define reference concentrations in molecule $\cdot$ m^{-3}: C_0 for species A, $C_{E_{Tot}}$ for E, and $k_1 C_{E_{Tot}} C_0/(k_{-1} + k_2)$ for EA (which is the maximum EA concentration for the Michaelis-Menten mechanism in a spatially homogenous environment; see [11]). We define reference distance L in m, and we let the reference number of molecules be equal to N_A molecules (i.e., emissions from the transmitter release one dimensionless molecule). We then define dimensionless concentrations as

$$C_a^\star = \frac{C_A}{C_0}, \quad C_e^\star = \frac{C_E}{C_{E_{Tot}}}, \quad C_{ea}^\star = \frac{C_{EA}(k_{-1} + k_2)}{k_1 C_{E_{Tot}} C_0}, \tag{5}$$

for species A, E, and EA, respectively. Similarly, dimensionless times are defined as

$$t_a^\star = \frac{D_A t}{L^2}, \quad t_e^\star = \frac{D_E t}{L^2}, \quad t_{ea}^\star = \frac{D_{EA} t}{L^2}, \tag{6}$$

and dimensionless coordinates along the three axes are

$$x^\star = \frac{x}{L}, \quad y^\star = \frac{y}{L}, \quad z^\star = \frac{z}{L}. \tag{7}$$

Fick's Second Law, which describes the motion of particles undergoing independent diffusion (see [12, Ch. 4]), can be written in dimensionless form for species S as

$$\frac{\partial C_s^\star}{\partial t_s^\star} = \nabla^2 C_s^\star, \tag{8}$$

where

$$\frac{\partial C_s^\star}{\partial t_s^\star} = \frac{\partial C_S}{\partial t}\frac{L^2}{D_S C_0}, \quad \nabla^2 C_s^\star = \frac{L^2}{C_0}\nabla^2 C_S. \tag{9}$$

By applying the principles of chemical kinetics (see [11, Ch. 9]) to the Michaelis-Menten mechanism in (1)-(3), the reaction-diffusion partial differential equations are

$$\frac{\partial C_A}{\partial t} = D_A\nabla^2 C_A - k_1 C_A C_E + k_{-1} C_{EA}, \tag{10}$$

$$\frac{\partial C_E}{\partial t} = D_E\nabla^2 C_E - k_1 C_A C_E + k_{-1} C_{EA} + k_2 C_{EA}, \tag{11}$$

$$\frac{\partial C_{EA}}{\partial t} = D_A\nabla^2 C_{EA} + k_1 C_A C_E - k_{-1} C_{EA} - k_2 C_{EA}, \tag{12}$$

and they can now be re-written in dimensionless form as

$$\frac{\partial C_a^\star}{\partial t_a^\star} = \nabla^2 C_a^\star - \gamma_{1a} C_e^\star C_a^\star + \gamma_{1a}\gamma_{2a} C_{ea}^\star, \tag{13}$$

$$\frac{\partial C_e^\star}{\partial t_e^\star} = \nabla^2 C_e^\star - \gamma_e C_e^\star C_a^\star + \gamma_e C_{ea}^\star, \tag{14}$$

$$\frac{\partial C_{ea}^\star}{\partial t_{ea}^\star} = \nabla^2 C_{ea}^\star + \gamma_{ea} C_e^\star C_a^\star - \gamma_{ea} C_{ea}^\star, \tag{15}$$

where

$$\gamma_{1a} = L^2 k_1 C_{E_{Tot}}/D_A, \quad \gamma_{2a} = k_{-1}/\left(k_{-1}+k_2\right), \tag{16}$$

$$\gamma_e = L^2 k_1 C_0/D_E, \quad \gamma_{ea} = L^2\left(k_{-1}+k_2\right)/D_{EA}, \tag{17}$$

are dimensionless constants. Generally, two system model parameter sets with all matching dimensionless constants are dimensionally homologous and will have the same dimensionless solutions; see [10].

III. Observations at the Receiver - Diffusion Only

In this section, we derive the expected number of A molecules counted within V_{obs} at time t for the cases of rectangular and spherical V_{obs}, given that the transmitter emits N_A molecules from the origin at $t = 0$ and there are no active enzymes. The local point concentration of A molecules at the point defined by vector $\vec{r}$ and at time $t > 0$ can be written in dimensionless form as [12, Eq. 4.28]

$$C_a^\star(\vec{r}_a^\star, t_a^\star) = \frac{1}{(4\pi t_a^\star)^{3/2}}\exp\left(\frac{-|\vec{r}_a^\star|^2}{4t_a^\star}\right), \tag{18}$$

where $\vec{r}_a^\star = \vec{r}/L$ is the vector defining dimensionless point $\{x^\star, y^\star, z^\star\}$ and we recall that one dimensionless molecule is emitted. Let $V_{obs}^\star$ be the dimensionless receiver volume, where each spatial dimension is scaled by L, and let $\overline{N_{a\,obs}^\star}(t)$ be the dimensionless expected (i.e., mean) number of observed A molecules. Thus, we need to solve

$$\overline{N_{a\,obs}^\star}(t) = \int\limits_{V_{obs}^\star} C_a^\star(\vec{r}_a^\star, t_a^\star) dV_{obs}^\star. \tag{19}$$

When applying the uniform concentration assumption, as we did in dimensional form in [9], we use $C_a^\star(\vec{r}_a^\star, t_a^\star) = C_a^\star(\vec{r}_{a,0}^\star, t_a^\star)\ \forall \vec{r}_a^\star$, where $\vec{r}_{a,0}^\star = \vec{r}_0/L$. Then,

$$\overline{N_{a\,obs}^\star}(t) = C_a^\star(\vec{r}_{a,0}^\star, t_a^\star) V_{obs}^\star, \tag{20}$$

since $C_a^\star(\vec{r}_{a,0}^\star, t_a^\star)$ does not vary over $V_{obs}^\star$.

A. Rectangular Volume

Let us first consider $V_{obs}^\star$ as a rectangular prism defined by $x_i^\star \le x^\star \le x_f^\star$ and analogously along $y^\star$ and $z^\star$. We present the following theorem:

Theorem 1 ($\overline{N_{a\,obs}^\star}(t)$ for Rectangular $V_{obs}^\star$): The expected number of A molecules counted within rectangular $V_{obs}^\star$ when one dimensionless molecule is released from the origin at $t_a^\star = 0$ is given by

$$\overline{N_{a\,obs}^\star}(t) = \int_{x_i^\star}^{x_f^\star}\int_{y_i^\star}^{y_f^\star}\int_{z_i^\star}^{z_f^\star} C_a^\star(\vec{r}_a^\star, t_a^\star) dz^\star dy^\star dx^\star \tag{21}$$

$$= \frac{1}{8}\prod_{\mathcal{D}\in\{x^\star,y^\star,z^\star\}}\left(\mathrm{erf}\left(\frac{\mathcal{D}_f}{2\sqrt{t_a^\star}}\right) - \mathrm{erf}\left(\frac{\mathcal{D}_i}{2\sqrt{t_a^\star}}\right)\right), \tag{22}$$

where $\mathcal{D} \in \{x^\star, y^\star, z^\star\}$ represents one of the dimensionless spatial variables, and the error function, $\mathrm{erf}\left(\cdot\right)$, is an odd function defined as [13, p. 406]

$$\mathrm{erf}\left(w\right) = \frac{2}{\sqrt{\pi}}\int_0^w \exp\left(-\mathcal{D}^2\right) d\mathcal{D}. \tag{23}$$

Proof: Using the substitution $v = \sqrt{b}\mathcal{D}$, it is straightforward to show that

$$\int_{\mathcal{D}_1}^{\mathcal{D}_2}\exp\left(-b\mathcal{D}^2\right)d\mathcal{D} = \frac{1}{2}\sqrt{\frac{\pi}{b}}\left(\mathrm{erf}\left(\sqrt{b}\mathcal{D}_2\right) - \mathrm{erf}\left(\sqrt{b}\mathcal{D}_1\right)\right). \tag{24}$$

We note that $|\vec{r}_a^\star|^2 = x^{\star 2} + y^{\star 2} + z^{\star 2}$, so (21) can be separated into three independent integrals. Using $b = \frac{1}{4t_a^\star}$, (22) follows. ∎

B. Spherical Volume

Next, we consider spherical $V_{obs}^\star$. In order to solve (19), we adjust our frame of reference so that the transmitter is emitting from the point defined by vector $\vec{r}_{x^\star}$ at $\{x_0^\star, 0, 0\}$, and the receiver volume $V_{obs}^\star$ with dimensionless radius $r_{obs}^\star$ is centered at the origin. The point defined by vector $\vec{r}_a^\star$ at $\{x^\star, y^\star, z^\star\}$ is still an arbitrary point in $V_{obs}^\star$. The distance from the source to $\vec{r}_a^\star$ is then $|\vec{r}_a^\star - \vec{r}_{x^\star}| = \sqrt{|\vec{r}_a^\star|^2 + |\vec{r}_{x^\star}|^2 - 2|\vec{r}_a^\star||\vec{r}_{x^\star}|\cos\phi\sin\theta}$, where $\phi = \tan^{-1}\left(y^\star/x^\star\right)$, $\theta = \cos^{-1}\left(z^\star/|\vec{r}_a^\star|\right)$, and $|\vec{r}_{x^\star}| = x_0^\star$. Thus, we need to solve

$$\overline{N_{a\,obs}^\star}(t) = \int_0^{r_{obs}^\star}\int_0^{2\pi}\int_0^{\pi} C_a^\star(\vec{r}_a^\star - \vec{r}_{x^\star}, t_a^\star)|\vec{r}_a^\star|^2\sin\theta d\theta d\phi d|\vec{r}_a^\star|, \tag{25}$$

where

$$C_a^\star(\vec{r}_a^\star - \vec{r}_{x^\star}, t_a^\star) = (4\pi t_a^\star)^{-\frac{3}{2}}\exp\left(\frac{-|\vec{r}_a^\star|^2 - |\vec{r}_{x^\star}|^2}{4t_a^\star}\right) \times \exp\left(\frac{|\vec{r}_a^\star||\vec{r}_{x^\star}|\cos\phi\sin\theta}{2t_a^\star}\right). \tag{26}$$

We now present the following theorem:

Theorem 2 ($\overline{N_{a\,obs}^\star}(t)$ for Spherical $V_{obs}^\star$): The expected number of A molecules counted within spherical $V_{obs}^\star$ when

one dimensionless molecule is released from $\vec{r}_{x^\star}$ at $t_a^\star = 0$ is given by

$$\overline{N_{a\,obs}^\star}(t) = \frac{1}{2}\left[\text{erf}\left(\frac{r_{obs}^\star - |\vec{r}_{x^\star}|}{2\sqrt{t_a^\star}}\right) + \text{erf}\left(\frac{r_{obs}^\star + |\vec{r}_{x^\star}|}{2\sqrt{t_a^\star}}\right)\right] + \frac{1}{|\vec{r}_{x^\star}|}\sqrt{\frac{t_a^\star}{\pi}}\left[\exp\left(-\frac{(|\vec{r}_{x^\star}| + r_{obs}^\star)^2}{4t_a^\star}\right) - \exp\left(-\frac{(|\vec{r}_{x^\star}| - r_{obs}^\star)^2}{4t_a^\star}\right)\right]. \quad (27)$$

Proof: Please refer to the Appendix. ∎

Due to symmetry, (27) applies to the general case of any spherical $V_{obs}^\star$ whose center is at a distance equal to $|\vec{r}_{x^\star}|$ from a point transmitter. Interestingly, also due to symmetry, (27) is analogous to the concentration at a *point receiver* due to a *spherical transmitter* releasing a uniform distribution of A molecules, as given in [14, Eq. 3.8]. A comparison between the expected number of observed molecules in spherical receivers with the number expected when we apply the uniform concentration assumption is made in Section V.

IV. Observations at the Receiver - Enzymes Present

In this section, we consider the presence of active enzymes. We have no analytical solution to the system of equations defined by (13)-(15). Following our reasoning applied in [9], where we used the uniform concentration assumption and assumed that $k_{-1}C_{EA} \to 0$ and $C_E \approx C_{E_{Tot}}$ (where $C_{E_{Tot}}$ is the dimensional total enzyme concentration), the lower bound on the expected concentration of molecules when enzymes are present can be written in dimensionless form as

$$C_a^\star \geq \frac{1}{(4\pi t_a^\star)^{3/2}} \exp\left(-\frac{L^2 k_1 C_{E_{Tot}}}{D_A} t_a^\star - \frac{|\vec{r}_{a,0}^\star|^2}{4t_a^\star}\right). \quad (28)$$

An explicit discussion of the accuracy of (28) would require a non-bounding expression for the expected number of molecules. We derived a lower bound, therefore we make a comparison between (13)-(15) and the system of partial differential equations that has (28) as its *exact* solution in order to make qualitative statements about the accuracy of (28). The latter system is

$$\left.\frac{\partial C_a^\star}{\partial t_a^\star}\right|_{\text{bound}} = \nabla^2 C_a^\star - \frac{L^2 k_1 C_{E_{Tot}}}{D_A} C_a^\star, \quad (29)$$

$$\left.\frac{\partial C_e^\star}{\partial t_e^\star}\right|_{\text{bound}} = 0, \quad (30)$$

$$\left.\frac{\partial C_{ea}^\star}{\partial t_{ea}^\star}\right|_{\text{bound}} = 0, \quad (31)$$

where $C_e^\star = 1$ is constant and $C_{ea}^\star = 0$. Unlike (13)-(15), this system of equations has a single dimensionless constant, $\gamma_{1a_{\text{bound}}}$,

$$\gamma_{1a_{\text{bound}}} = L^2 k_1 C_{E_{Tot}}/D_A = \gamma_{1a}. \quad (32)$$

The accuracy of (28) in dimensionless form can then be written as the differences between (13)-(15) and (29)-(31), i.e.,

$$\left.\frac{\partial C_a^\star}{\partial t_a^\star} - \frac{\partial C_a^\star}{\partial t_a^\star}\right|_{\text{bound}} = \frac{L^2}{D_A} C_{EA}\left(\frac{k_{-1}}{C_0} + k_1 C_a^\star\right), \quad (33)$$

$$\left.\frac{\partial C_e^\star}{\partial t_e^\star} - \frac{\partial C_e^\star}{\partial t_e^\star}\right|_{\text{bound}} = \nabla^2 C_e^\star - \gamma_e C_e^\star C_a^\star + \gamma_e C_{ea}^\star, \quad (34)$$

$$\left.\frac{\partial C_{ea}^\star}{\partial t_{ea}^\star} - \frac{\partial C_{ea}^\star}{\partial t_{ea}^\star}\right|_{\text{bound}} = \nabla^2 C_{ea}^\star + \gamma_{ea} C_e^\star C_a^\star - \gamma_{ea} C_{ea}^\star, \quad (35)$$

where we used $C_{E_{Tot}} = C_E + C_{EA}$, even though $C_{E_{Tot}}$ was not defined as a function of time and space. Of course, (34) and (35) are identical to (14) and (15), respectively. Eqs. (33)-(35) show what we lose when we consider the lower bound (28). Particularly, we lose all of the reaction-diffusion dynamics of the E and EA molecules. Eqs. (34) and (35) have both positive and negative terms, so we focus on (33) to make comments about the accuracy of (28). This is acceptable because we are ultimately most interested in the dynamics of the A molecules.

From (33), we can immediately claim:

1) A higher k_1, k_{-1}, or an increase in N_A or N_E in an otherwise unchanged system will decrease the accuracy of (28), because having more A or E molecules indirectly increases C_{EA}.
2) A higher k_2 in an otherwise unchanged system will increase the accuracy of (28), because there will be fewer EA molecules throughout the system. This observation is also intuitive given that $k_2 \to \infty$ leads to our assumption that $k_{-1}C_{EA} \to 0$.
3) The impact of scaling L and D_A is non-trivial because both $C_a^\star$ and C_{EA} are functions of location. A larger L or smaller D_A might decrease the accuracy of (28), but increasing L or decreasing D_A would also mean that the observed $C_a^\star$ and C_{EA} decrease, which we have already said would increase the accuracy.

The cumulative impact on the accuracy of (28) when varying the environmental parameters is better appreciated with simulations, as we present in Section V.

V. Numerical and Simulation Results

A. Uniform Concentration Assumption

We first present a numerical test of the uniform concentration assumption. We set $L = \vec{r}_0$; we are only interested in $r_{obs}^\star < 1$. Small values of $r_{obs}^\star$ correspond to a smaller receiver or the receiver placed further from the transmitter. In Fig. 1, we show how much $\overline{N_{a\,obs}^\star}(t)$ at a spherical receiver of radius $r_{obs}^\star$ deviates from the true value over time when we assume that the concentration throughout $V_{obs}^\star$ is uniform. A similar test was also performed for the deviation at a cube, and the results were visually indistinguishable to Fig. 1 so they are omitted here due to space (though they show that the exact shape of $V_{obs}^\star$ is not important).

We see in Fig. 1 that the deviation from the true value of $\overline{N_{a\,obs}^\star}(t)$ increases with $r_{obs}^\star$. There is significant deviation for any $r_{obs}^\star$ when $t_a^\star$ is sufficiently small. $\overline{N_{a\,obs}^\star}(t)$ is underestimated for all $r_{obs}^\star$ until $t_a^\star \approx 0.16$ and then it is overestimated,

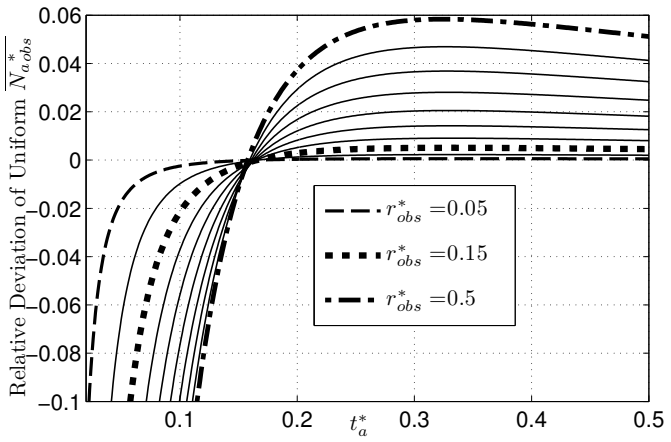

Fig. 1. The relative deviation in $\overline{N_{a\,obs}^{\star}}(t)$ from the true value (27) at a spherical receiver when the uniform concentration assumption (20) is applied without active enzymes. The deviation is evaluated as ((20)-(27))/(27). The spherical receiver radius $r^{\star}_{obs}$ is increased in increments of 0.05, where a larger $r^{\star}_{obs}$ results in a larger deviation.

but the deviation tends to 0 as $t_a^{\star} \to \infty$. This transition is intuitive; molecules tend to diffuse to the edge of $V^{\star}_{obs}$ before they reach the center. However, the centre of $V^{\star}_{obs}$ is closer to the transmitter than most of $V^{\star}_{obs}$, leading to the eventual overestimate of $\overline{N_{a\,obs}^{\star}}(t)$.

The deviation in $\overline{N_{a\,obs}^{\star}}(t)$ should be no more than a few percent. We are generally interested in values of $t_a^{\star} > 0.1$, so the initial large deviation for all values of $r^{\star}_{obs}$ is not a major concern. Small values of $r^{\star}_{obs}$, i.e., $r^{\star}_{obs} \leq 0.15$, maintain a deviation of less than $2\,\%$ for all $t_a^{\star} > 0.1$. Thus, we claim that the uniform concentration assumption is sufficient when studying receivers whose radius is no more than $15\,\%$ of the distance from the center of the receiver to the transmitter.

B. Dimensionless Accuracy of Expected Number of Molecules

We now consider two systems with different environmental parameters in order to assess the accuracy of the lower bound expression (28) and highlight the scalability of the dimensionless model. The details of our particle-based simulation framework are described in [9]. We assume that each system has a viscosity of $10^{-3}\,\mathrm{kg\,m^{-1}s^{-1}}$ and temperature of $25\,^{\circ}\mathrm{C}$. V_{enz} is defined as a cube with side length $1\,\mu$m, and centered at the origin. We set simulation time step $\Delta t = 0.5\,\mu$s. The reference parameters are $L = |\vec{r}_0| = 300/\sqrt{2}\,$nm and $C_0 = \frac{N_A}{1\,\mathrm{m}^3}$. Each system has a spherical receiver with dimensionless radius $r^{\star}_{obs} = 0.15$. The radii of the molecular species are $R_A = 0.5\,$nm, $R_E = 2.5\,$nm, and $R_{EA} = 3\,$nm. The rate constants k_{-1} and k_2 are $2\times10^4\,\mathrm{s}^{-1}$ and $2\times10^6\,\mathrm{s}^{-1}$, respectively. The unique system parameters are described in Table I. The number of molecules and the size of the environments are kept deliberately low to ease simulation time.

One can quickly verify that the two systems are dimensionally homologous according to the constants in (16)-(17). They have the same lower bound on the expected number of observed molecules as defined by (28), and have the same loss in accuracy as defined by (33) when we use $k_1 C_{E_{Tot}} C_0/(k_{-1}+k_2)$ for C_{EA} and 1 in place of $C_a^{\star}$.

TABLE I
SYSTEM PARAMETERS USED FOR FIG. 2.

Parameter	System 1	System 2
N_A	10^4	2×10^4
$N_{E_{Tot}}$	2×10^5	4×10^5
k_1 $[\frac{\mathrm{m}^3}{\mathrm{molecule\cdot s}}]$	2×10^{-19}	10^{-19}

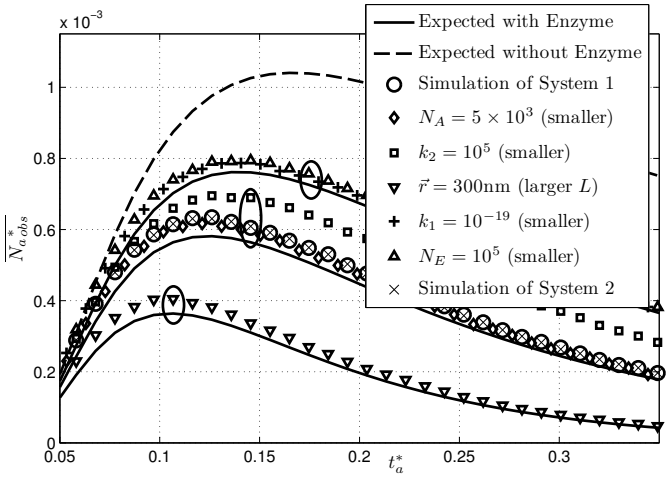

Fig. 2. Assessing 1) the accuracy of the lower bound on the expected number of observed information molecules and 2) the consistency of dimensionally homologous systems. Systems 1 and 2 are dimensionally homologous and the modified versions of System 1 are not, although many share common lower bounds on $\overline{N_{a\,obs}^{\star}}(t)$ (as grouped by ellipses). The units for the modified rate constants are the same as those listed in the text and in Table I. For reference, the maximum dimensional expected number of molecules observed for Systems 1 and 2 when enzymes are present is 5.81 and 11.63 molecules at $12.84\,\mu$s, respectively.

In Fig. 2, we compare the observed number of dimensionless molecules using the two sets of system parameters, in addition to variations of System 1 with a single parameter modified (as noted in the legend, and these variations are not homologous). The number of A molecules observed via simulation is averaged over at least 6000 independent emissions by the transmitter at $t_a^{\star} = 0$. We measure the dimensionless number of information molecules observed over dimensionless time, in comparison to the lower bound expression (28) and the expected number without enzymes in the environment as given by (28) for $C_{E_{Tot}} = 0$ (where in both cases the concentrations given by (28) are multiplied by $V^{\star}_{obs}$).

We clearly see in Fig. 2 that the receivers in Systems 1 and 2 observe, on average, the same number of dimensionless information molecules. The changes in accuracy for the modified versions of System 1 are consistent with the claims made from (33); the accuracy of (28) improves with lower N_A, N_E, k_1, or higher k_2. With an increase in L, the accuracy appears to be worse initially and then improves more rapidly over time. Importantly, $\overline{N_{a\,obs}^{\star}}(t)$ as shown in most curves is much closer to the lower bounds than to the expected value without enzymes (without enzymes, all systems here have the same $\overline{N_{a\,obs}^{\star}}(t)$).

This accuracy is achieved even though these systems have a high k_1 value (the largest possible value of k_1 is on the order of 1.66×10^{-19} molecule^{-1}m^3 s^{-1}; see [11, Ch. 10]) and a large enzyme concentration (the lowest concentration considered here, 166 μM when System 1 is modified so that $N_{E_{Tot}} = 10^5$, is still high for a cellular enzyme; see [15]). Thus, the lower bound expression (28) can be applied in future work to derive communications performance when enzymes are added to mitigate ISI. Furthermore, the dimensional analysis enables us to simulate small environments, even if they are too small for a practical implementation with modern technology, and then scale the results to arbitrarily larger but dimensionally homologous environments with many more molecules, thereby saving computational resources.

VI. Conclusions

In this paper, we used dimensional analysis to study a diffusive molecular communication system where diffusing enzymes in the propagation environment mitigate intersymbol interference. We derived the exact expected number of information molecules observed at cubic and spherical receivers when enzymes are not present, and showed that the uniform concentration assumption is sufficiently accurate when the radius of the receiver is no more than 15 % of the distance from the transmitter to the center of the receiver. We also showed that, when active enzymes are present, the accuracy of the lower bound expression on the expected number of molecules can be qualitatively described with respect to the environmental parameters. Adopting a dimensionless model saves computational resources for analytical verification by simulating environments with fewer molecules. On-going work is using the lower bound to assess the design of practical signal detection schemes for the receiver in such an environment with derivation of the corresponding bit error probabilities to more clearly demonstrate the improvement in communication performance when using enzymes.

Appendix

To prove Theorem 2, we first integrate (25) with respect to ϕ by using [16, Eq. 3.339]

$$\int_0^{\pi} \exp\left(b\cos w\right) dw = \pi I_0(b)\,, \tag{36}$$

where $I_0(b)$ is the modified zeroth order Bessel function of the first kind. It is straightforward to show that the integral of $\exp\left(b\cos w\right)$ from $w = \pi$ to $w = 2\pi$ is also $\pi I_0(b)$, so from (25) we can write

$$\int_0^{2\pi} \exp\left(\frac{|\vec{r}_a^{\star}||\vec{r}_{x^\star}|\cos\phi\sin\theta}{2t_a^\star}\right) d\phi = 2\pi I_0\left(\frac{|\vec{r}_a^{\star}||\vec{r}_{x^\star}|\sin\theta}{2t_a^\star}\right). \tag{37}$$

Next, we integrate with respect to θ by using [16, Eq. 6.681.8]

$$\int_0^{\pi} \sin\left(2\mu w\right) J_{2\nu}(2b\sin w)\, dw = \pi \sin\left(\mu\pi\right) J_{\nu-\mu}(b)\, J_{\nu+\mu}(b)\,, \tag{38}$$

where $J_i(b)$ is the ith order Bessel function of the first kind and $I_0(b) = J_0(jb)$, where $j = \sqrt{-1}$. From (25), (37), and (38) we can write

$$\int_0^{\pi} \sin\theta I_0\left(\frac{|\vec{r}_a^{\star}||\vec{r}_{x^\star}|\sin\theta}{2t_a^\star}\right) d\theta = \pi J_{-\frac{1}{2}}\left(\frac{j|\vec{r}_a^{\star}||\vec{r}_{x^\star}|}{4t_a^\star}\right) J_{-\frac{1}{2}}\left(\frac{j|\vec{r}_a^{\star}||\vec{r}_{x^\star}|}{4t_a^\star}\right). \tag{39}$$

Using [16, Eqs. 1.311, 1.334, 8.464.1-2], it is straightforward to show that

$$J_{-\frac{1}{2}}(jb)\, J_{\frac{1}{2}}(jb) = \frac{1}{2\pi b}\left(\exp\left(2b\right) - \exp\left(-2b\right)\right), \tag{40}$$

so (25) is now reduced to

$$\overline{N_{a\,obs}^{\star}}(t) = \frac{1}{2|\vec{r}_{x^\star}|\sqrt{\pi t_a^\star}} \int_0^{r_{obs}^\star} |\vec{r}_a^{\star}| \left[\exp\left(-\frac{\left(|\vec{r}_{x^\star}| - |\vec{r}_a^{\star}|\right)^2}{4t_a^\star}\right) - \exp\left(-\frac{\left(|\vec{r}_{x^\star}| + |\vec{r}_a^{\star}|\right)^2}{4t_a^\star}\right)\right] d|\vec{r}_a^{\star}|, \tag{41}$$

which can be solved using substitution to arrive at (27). ■

References

[1] B. Alberts, D. Bray, K. Hopkin, A. Johnson, J. Lewis, M. Raff, K. Roberts, and P. Walter, *Essential Cell Biology*, 3rd ed. Garland Science, 2010.

[2] I. F. Akyildiz, F. Brunetti, and C. Blazquez, "Nanonetworks: A new communication paradigm," *Computer Networks*, vol. 52, no. 12, pp. 2260–2279, May 2008.

[3] T. Nakano, M. J. Moore, F. Wei, A. V. Vasilakos, and J. Shuai, "Molecular communication and networking: Opportunities and challenges," *IEEE Trans. Nanobiosci.*, vol. 11, no. 2, pp. 135–148, Jun. 2012.

[4] S. Kadloor, R. R. Adve, and A. W. Eckford, "Molecular communication using Brownian motion with drift," *IEEE Trans. Nanobiosci.*, vol. 11, no. 2, pp. 89–99, Jun. 2012.

[5] B. Atakan and O. B. Akan, "Deterministic capacity of information flow in molecular nanonetworks," *Nano Commun. Net.*, vol. 1, no. 1, pp. 31–42, Mar. 2010.

[6] A. Einolghozati, M. Sardari, A. Beirami, and F. Fekri, "Capacity of discrete molecular diffusion channels," in *Proc. 2011 IEEE ISIT*, Aug. 2011, pp. 723–727.

[7] M. U. Mahfuz, D. Makrakis, and H. T. Mouftah, "A comprehensive study of concentration-encoded unicast molecular communication with binary pulse transmission," in *Proc. 2011 IEEE NANO*, Aug. 2011, pp. 227–232.

[8] B. Atakan, S. Galmes, and O. B. Akan, "Nanoscale communication with molecular arrays in nanonetworks," *IEEE Trans. Nanobiosci.*, vol. 11, no. 2, pp. 149–160, Jun. 2012.

[9] A. Noel, K. C. Cheung, and R. Schober, "Improving diffusion-based molecular communication with unanchored enzymes," in *Proc. 2012 ICST BIONETICS*, Dec. 2012. [Online]. Available: ece.ubc.ca/~adamn/pub.html

[10] T. Szirtes, *Applied Dimensional Analysis and Modeling*, 2nd ed. Butterworth-Heinemann, 2007.

[11] R. Chang, *Physical Chemistry for the Biosciences*. University Science Books, 2005.

[12] P. Nelson, *Biological Physics: Energy, Information, Life*, updated 1st ed. W. H. Freeman and Company, 2008.

[13] K. B. Oldham, J. C. Myland, and J. Spanier, *An Atlas of Functions with Equator, the Atlas Function Calculator*, 2nd ed. Springer, 2008.

[14] J. Crank, *The Mathematics of Diffusion*, 2nd ed. Oxford University Press, 1980.

[15] K. R. Albe, M. H. Butler, and B. E. Wright, "Cellular concentrations of enzymes and their substrates," *J. Theor. Biol.*, vol. 143, no. 2, pp. 163–195, Mar. 1990.

[16] I. S. Gradshteyn and I. M. Ryzhik, *Table of Integrals, Series, and Products*, 5th ed. London: Academic Press, 1994.